J. Fluid Mech. (1976), *vol.* 77, *part* 3, *pp.* 511–529
Printed in Great Britain

The spatial viscous instability of axisymmetric jets

By PHILIP J. MORRIS
Lockheed-Georgia Company, Marietta, Georgia

(Received 25 October 1974 and in revised form 15 June 1976)

The stability of three axisymmetric jet profiles is reviewed. These profiles represent the development of an incompressible jet from a nearly top-hat profile to a fully developed jet profile. The disturbance equations for arbitrary mode number in a region of zero shear, which provide the boundary conditions for the numerical solution, are solved analytically through use of the disturbance vorticity equations. Numerical solutions for the spatial stability for the axisymmetric ($n = 0$) disturbance and the asymmetric $n = 1$ disturbance are presented. Previously published calculations of least stable modes are shown to be incorrectly interpreted and their actual mode types are given. The critical Reynolds number is found to increase as the profile varies from a top-hat to a fully developed jet form. Closed contours of constant amplification, which are unusual in free shear flows, are shown to exist for the $n = 1$ disturbance in the fully developed jet region. A fluctuation energy balance is used to justify the occurrence of this destabilizing effect of decreasing Reynolds number.

1. Introduction

Though the axisymmetric jet is known to be unstable at high Reynolds numbers the experimental observations of the characteristic disturbances do not provide a consistent description of the instability process. Reynolds (1962) reported modes of instability of a dyed water jet submerged in a water tank. These modes included axisymmetric condensations for Reynolds numbers, based on the volume flow at the jet exit, in the range 50–250 and sinuous, long wavelength undulations for Reynolds numbers of 100–250. Above a Reynolds number of 300 only a confused breakup was observed. Viilu (1962), in a similar experiment, found a critical Reynolds number between 10·5 and 11·8. In more recent experiments, Mattingly & Chang (1974) showed for a Reynolds number of 300 that close to the jet exit the axisymmetric mode dominated whereas further downstream, where the shear-layer half-width was 55 % of the potential-core radius, the disturbance observed experimentally exhibited an axisymmetric character half the time and a helical one the rest of the time.

There have been a number of analytical studies which have attempted to describe the stability characteristics of the axisymmetric jet. In many cases, the essential stability characteristics of a flow are revealed by inviscid stability calculations. Batchelor & Gill (1962) and Mattingly & Chang (1974) both considered only the inviscid stability of the jet flow. Batchelor & Gill (1962) considered a 'top-hat' velocity profile to represent the mean flow close to the jet

exit. Crighton (1973) indicated that real velocity profiles do not have this character except close to the nozzle, where the effect of the nozzle cannot be ignored (see Orszag & Crow 1970). Mattingly & Chang (1974) and Michalke (1971) showed that good agreement with experimental results could be obtained assuming spatial growth of the disturbances and realistic mean velocity profiles. (Michalke considered the turbulent jet excitation experiments by Crow & Champagne 1971.) Thus it may be concluded that the use of realistic mean velocity profiles is important in the stability calculations. The disadvantage of using a realistic profile is that in most cases the stability calculations must be performed numerically since no simple analytic eigenvalue equation exists.

The stability of viscous axisymmetric flows has received little attention in comparison with that of plane flows. Gill (1962) used a simplified viscous analysis to attempt to explain the occurrence of axisymmetric growing disturbances in the developed axisymmetric jet. His analysis (1965) of axisymmetric pipe flow was also confined to the $n = 0$, axisymmetric mode. Lessen, Sadler & Liu (1968), Garg (1971) and Garg & Rouleau (1972) have provided an extensive study of the spatial stability of pipe Poiseuille flow. They considered a viscous fluid and found solutions numerically for arbitrary azimuthal mode numbers.

Recently the problem of the viscous stability of a round jet has been studied by several workers. Burridge (1968) considered temporal amplification only and obtained numerical solutions for a jet velocity profile given by $u = (1+r^2)^{-2}$. Kambe (1969) also considered the temporal instability of a round jet with a discontinuous parabolic mean velocity profile. Mollendorf & Gebhart (1973) and Lessen & Singh (1973) have recently studied the viscous spatial stability of a jet with the same profile as that used by Batchelor & Gill (1962) and Burridge (1968).

The present paper describes the viscous spatial stability of an axisymmetric jet to disturbances of arbitrary azimuthal mode number. Jet velocity profiles characterizing several stages of development of a round jet are examined. In this manner the axial development of a disturbance of fixed frequency may be examined.

2. Stability equations and boundary conditions

The four coupled ordinary differential equations for the disturbance motion have been derived by Batchelor & Gill (1962). The velocity and pressure are decomposed into a steady mean flow and superimposed disturbances. The equation of motion linear in the disturbances in tensor form is

$$\partial u_i^*/\partial t^* + U^* u_{i,3}^* + u_1^* U_{,1}^* \delta_i^3 = -\rho^{-1} p_{,i}^* + \nu^* [u_{i,}^{*j}]_{,j}, \tag{2.1}$$

where the disturbance velocity tensor u_i^* has physical velocity components v^*, $w^* r^*$ and u^* with respect to the cylindrical co-ordinates r^*, ϕ and z^* and the axial velocity component of the axisymmetric parallel mean flow is $U^*(r^*)$. The usual notation for covariant differentiation has been used. The disturbance continuity equation is

$$u^{*j}{}_{,j} = 0. \tag{2.2}$$

The disturbance is assumed to Fourier decompose into complex components typically of the form

$$\phi^*(r^*, \phi, z^*, t^*) = \mathrm{Re}\,[\hat{\phi}^*(r^*)\exp\{i(\alpha^* z^* - \omega^* t^* + n\phi)\}], \tag{2.3}$$

where α^* is the complex wavenumber, ω^* is the real radian frequency and n is the azimuthal mode number. Substituting terms of the form (2.3) for the velocity and pressure fluctuations into (2.2) and (2.1), we obtain four coupled ordinary differential equations for the four unknown functions $\hat{v}^*$, $\hat{w}^*$, $\hat{u}^*$ and $\hat{p}^*$. Non-dimensionalizing these coupled differential equations with respect to a velocity scale V_c^*, a length scale L_c^* and the ambient density ρ_0^* and introducing the Reynolds number $R = U_c^* L_c^*/\nu_0^*$, these equations can be written as

$$i\alpha\hat{u} + \hat{v}' + \hat{v}/r + in\,\hat{w}/r = 0, \tag{2.4}$$

$$i\alpha(U-c)\,\hat{v} + \hat{p}' = \frac{1}{R}\left[\hat{v}'' + \frac{\hat{v}'}{r} - \left\{\alpha^2 + \frac{(n^2+1)}{r^2}\right\}\hat{v} - i\frac{2n}{r^2}\hat{w}\right], \tag{2.5}$$

$$i\alpha(U-c)\,\hat{w} + \frac{in}{r}\hat{p} = \frac{1}{R}\left[\hat{w}'' + \frac{\hat{w}'}{r} - \left\{\alpha^2 + \frac{(n^2+1)}{r^2}\right\}\hat{w} + i\frac{2n}{r^2}\hat{v}\right] \tag{2.6}$$

and

$$i\alpha(U-c)\,\hat{u} + U'\hat{v} + i\alpha\hat{p} = \frac{1}{R}\left[\hat{u}'' + \frac{\hat{u}'}{r} - \left\{\alpha^2 + \frac{n^2}{r^2}\right\}\hat{u}\right], \tag{2.7}$$

where $c = \omega/\alpha$ and primes denote differentiation with respect to r.

The boundary conditions on the fluctuations are (Batchelor & Gill 1962)

$$\hat{v}, \hat{w}, \hat{u}, \hat{p} \to 0 \quad \text{as} \quad r \to \infty \tag{2.8}$$

and

$$\hat{u}(0) = \hat{p}(0) = 0, \quad n \neq 0, \tag{2.9}$$

$$\hat{v}(0) = \hat{w}(0) = 0, \quad n \neq 1, \tag{2.10}$$

$$\hat{v}(0) + i\hat{w}(0) = 0, \quad n = 1. \tag{2.11}$$

In order to develop the numerical technique for solution of these equations it is necessary to find the form of the solutions close to the axis of symmetry and in the nearly undisturbed fluid surrounding the jet. These asymptotic solutions will be developed in the next section.

3. Asymptotic solutions of the stability equations

Inspection of the stability equations (2.4)–(2.7) reveals that for $n = 0$, i.e. axisymmetric disturbances, the sixth-order set of equations can be separated into one fourth-order and one second-order set of equations. The fourth-order set contains only radial and axial velocity components. Because of this simplification it is convenient to look at the cases of axisymmetric disturbances, $n = 0$, and asymmetric disturbances, $n \neq 0$, separately.

Axisymmetric disturbances: $n = 0$

For small values of r, Lessen *et al.* (1968) and Garg (1971) obtained the solution to the disturbance equations by expanding the velocity and pressure fluctuations in a power series in r. The recurrence relations for the coefficients in the

power-series expansion are given by Garg (1971). The eigenfunctions can then be expressed as the sum of two linearly independent solutions. The fourth-order system of differential equations the $n = 0$ disturbance may be reduced to a single fourth-order equation for the transverse velocity fluctuation $\hat{v}$. Sufficiently far from the jet axis the terms involving derivatives of the mean flow are negligible. If a first-order Hankel transformation is performed on this fourth-order equation in terms of a radial wavenumber k, a quartic equation for k is obtained. Thus the form of the solution for $\hat{v}$ outside the jet in a region of constant mean flow is found to be

$$\hat{v} = A_1 H_1^{(1)}(i\alpha r) + A_2 H_1^{(2)}(i\alpha r) + A_3 H_1^{(1)}(i\beta r) + A_4 H_1^{(2)}(i\beta r), \tag{3.1}$$

where $\beta = [\alpha^2 + i\alpha R(U_0 - c)]^{\frac{1}{2}}$, and U_0 is a constant mean flow velocity far from the jet axis. In order to satisfy the boundary conditions as $r \to \infty$, only two of the solutions of (3.1) for $\hat{v}$ can be retained. The choice of the Hankel function of the first or second kind depends on the phase of their arguments.

Asymmetric disturbances: $n \neq 0$

For asymmetric disturbances the eigenfunctions may again be expanded as a power series for small r. The corresponding recurrence relations for the coefficients in the series expansion are given by Garg & Rouleau (1972). In a manner similar to that for the case $n = 0$, it can be shown that the solution can be expressed in terms of three independent solutions.

The analytical solution of the stability equations (2.4)–(2.7) in a region of constant mean velocity has been derived by Kambe (1969) and Burridge (1968). In the former work the solution was derived in terms of $T(r) = -i(\hat{v} + i\hat{w})$ $S(r) = -i(\hat{v} - i\hat{w})$, while Burridge introduced the new variables

$$\phi = i\hat{v}r, \quad \Omega = (\alpha r\hat{w} - n\hat{u})/(n^2 + \alpha^2 r^2).$$

However, the form of the solutions for the velocity and pressure fluctuations is more conveniently derived if the vorticity equations are considered. The components of the fluctuating vorticity vector ω are assumed to take the form

$$\{\omega_1, \omega_2, \omega_3\}(r, \phi, z, t) = \mathrm{Re}\,[\{\hat{r}_1, \hat{r}_2, \hat{r}_3\}(r) \exp\{i(\alpha z - \omega t + n\phi)\}]. \tag{3.2}$$

If new dependent variables

$$\hat{s} \equiv \hat{r}_1 + i\hat{r}_2, \quad \hat{t} \equiv \hat{r}_1 - i\hat{r}_2 \tag{3.3}$$

are introduced, it may then be readily shown that the solutions for $\hat{s}$, $\hat{t}$ and r_3 take the form

$$\left.\begin{aligned} \hat{s}(r) &= S_{1,2} H_{n+1}^{(1),(2)}(i\beta r), \\ \hat{t}(r) &= T_{1,2} H_{n-1}^{(1),(2)}(i\beta r), \\ \hat{r}_3(r) &= R_{1,2} H_n^{(1),(2)}(i\beta r), \end{aligned}\right\} \tag{3.4}$$

where a Hankel function of the first or second kind is chosen, depending on the argument, such that the boundary conditions on the disturbances are met. The $\hat{r}_1$ and $\hat{r}_2$ vorticity components can be obtained using (3.3). One of the three remaining constants in (3.4) may be eliminated using the fact that the divergence

of the vorticity is zero. By making use of the relationship between the vorticity and velocity components and using the z-momentum equation to obtain the pressure fluctuation, the asymptotic form, for large radii of the velocity and pressure disturbances can be shown to be

$$\hat{u} = A_{1,2} H_n^{(1),(2)}(i\alpha r) + A_{3,4} H_n^{(1),(2)}(i\beta r), \tag{3.5a}$$

$$\hat{v} = -A_{1,2} \frac{\mathrm{i}}{\alpha} \frac{d}{dr} \{H_n^{(1),(2)}(i\alpha r)\} + A_{3,4} \frac{\alpha}{\beta} H_{n+1}^{(1),(2)}(i\beta r) - A_{5,6} \frac{in}{\beta r} H_n^{(1),(2)}(i\beta r), \tag{3.5b}$$

$$\hat{w} = A_{1,2} \frac{n}{\alpha r} H_n^{(1),(2)}(i\alpha r) + A_{3,4} \frac{i\alpha}{\beta} H_{n+1}^{(1),(2)}(i\beta r) + A_{5,6} \frac{1}{\beta} \frac{d}{dr} \{H_n^{(1),(2)}(i\beta r)\} \tag{3.5c}$$

and

$$\hat{p} = A_{1,2}(\omega/\alpha - U_0) H_n^{(1),(2)}(i\alpha r). \tag{3.5d}$$

The solutions (3.5) represent the form of the solutions in any region where the mean velocity is constant and it can be shown that these solutions are equivalent to the series expansions by Garg & Rouleau for small r, where modified Bessel functions of the first kind replace the Hankel functions. Such a solution would be valid in the potential core of a round jet.

The expansions and analytic solutions derived in this section will form the basis of the numerical technique described in the next section.

4. Numerical method of solution of eigenvalue problem

Since the numerical techniques for the axisymmetric and asymmetric disturbances are very similar, we shall discuss here only the technique for the more complex problem of asymmetric disturbances.

For small r the eigensolutions can be determined using the power-series expansion and the recurrence relationships if the mean velocity is not constant or a solution of the form (3.5) if the mean velocity is constant. These solutions provide the starting conditions for step-by-step numerical integration at $r = r_s$. Equations (2.4)–(2.7) may be written as six first-order differential equations in the dependent variables $\hat{v}$, $\hat{w}$, $\hat{u}$, $\hat{p}$, $D\hat{u}$ and $\hat{D}\hat{w}$. The three independent solutions are integrated numerically using a standard Runge–Kutta scheme with error minimization developed by Fyfe (1966). In order to preserve the linear independence of the three solutions, a normalization and orthogonalization procedure is performed at a number of steps within the range of the numerical integration. This method is discussed by Bellman & Kalaba (1965, p. 98) and Davey (1973). The technique has been successfully applied by Sharma (1968), Davey & Nguyen (1971) and Morris (1971) among others. It is the simplest and most accurate method of decontaminating the linear solutions. In the integration used in this work the modifications proposed by Conte (1966) have been employed. In this technique an orthonormalization is applied when the angle between the independent vectors is too small or when the magnitude of any vector exceeds a pre-assigned constant whose size is determined by the magnitude of the expected solution. Conte showed that the optimum choice of the minimum angle between vectors is surprisingly small, of the order of 1°, since accuracy is lost by too

frequent orthonormalization because of the extensive matrix and vector multiplications which are required.

The numerical solutions at some location $r = a$ in the uniform flow outside the jet are of the form

$$\hat{u}(a) = G_1 \hat{u}_1(a) + U_1 \hat{u}_2(a) + P_1 \hat{u}_3(a). \tag{4.1}$$

The six coefficients in (4.1) and (3.5) may be found by elimination of the six dependent variables at $r = a$, which leads to

$$\mathbf{F}(\alpha, \omega, R)\,[A_{1,2}, A_{3,4}, A_{4,5}, U_1, G_1, P_1]^{\mathrm{T}} = 0, \tag{4.2}$$

where $\mathbf{F}(\alpha, \omega, R)$ is a 6×6 matrix whose coefficients may easily be found from (3.5) and (4.1). The eigenvalues can then be determined by satisfying the condition

$$\Delta \equiv \det \mathbf{F} = 0. \tag{4.3}$$

An iterative technique is used to determine an eigenvalue. An nth-order inverse Lagrangian interpolation scheme is used to minimize Δ, and the $(n+1)$th guess α_{n+1} for the eigenvalue is given by

$$\alpha_{n+1} = \sum_{j=0}^{n} \alpha_j (-1)^n \prod_{\substack{i=0 \\ i \neq j}}^{n} \Delta_i / \prod_{\substack{i=0 \\ i \neq j}}^{n} (\Delta_j - \Delta_i). \tag{4.4}$$

The convergence to an eigenvalue is much improved if the initial guesses are as accurate as possible. The original location of an eigenvalue was determined using the technique employed by Lessen *et al.* (1968). In their technique the number of eigenvalues within a closed contour is established by determining the net multiples of 2π by which the phase of the determinant Δ changes around the contour. This method is extremely powerful since, as will be seen later, it avoids the possibility of missing the least stable eigenvalue. In the next section the mean velocity profiles will be examined.

5. Mean velocity profiles in the jet

Before performing the numerical solution of the stability equations, it is necessary to specify the mean velocity profile. Although the mean flow is diverging the solutions to be presented here are based on the assumption that the flow is locally parallel. The choice of mean profiles has been governed by available experimental evidence and by the wish to enable a comparison with other theoretical solutions.

The solution of Landau & Lifshitz (1959, p. 86) of the boundary-layer equations for a similar axisymmetric jet issuing from a small orifice, which will be called profile I, is given by

$$U^*/U_c^* = \{1 + r^{*2}/r_0^{*2}\}^{-2}, \tag{5.1}$$

where $r_0^* = 8x/R$, $U_c^* = \nu R^2/8x$ and $R = (3M/\pi\mu\nu^2)^{\frac{1}{2}}$ for small angles of spread of the jet, M being the flux of momentum across a plane normal to the jet axis. The form (5.1) for the mean profile corresponds to that used by Burridge (1968) and Lessen & Singh (1973). The experiments by Andrade & Tsien (1937) and

the numerical results of Pai & Hsieh (1972) show that the mean velocity profiles approach the form (5.1) far from the jet orifice. Thus the solutions for this profile will represent the stability of the axisymmetric fully developed jet.

Close to the jet exit the mean velocity profile may approach a top-hat profile. On the basis of Freymuth's (1966) experiments Michalke (1971) used two velocity profiles to describe the transition from a top-hat profile at the jet exit to the fully developed jet profile (5.1). The first velocity profile, referred to as profile II, is given by

$$\frac{U^*}{U_c^*} = \begin{cases} 1, & 0 \leqslant r < 1-\frac{1}{2}\delta, \\ \frac{1}{2}\{1+\tanh[(1-r)/2\theta]\}, & 1-\frac{1}{2}\delta < r < \infty, \end{cases} \tag{5.2}$$

where δ is chosen such that $\tanh(\delta/4\theta)$ is close to unity to minimize the discontinuity in the profile at $r = 1-\frac{1}{2}\delta$. θ is the local momentum thickness, defined by

$$\theta = \int_0^\infty U(1-U)\,dr, \tag{5.3}$$

and can be used to represent the influence of axisymmetry on the stability of the jet.

The second velocity profile, referred to as profile III, is given by

$$\frac{U^*}{U_c^*} = \frac{1}{2}\left\{1+\tanh\left[\frac{1}{4\theta}\left(\frac{1}{r}-r\right)\right]\right\} \tag{5.4}$$

and is taken to be representative of the mean velocity profile in the region towards the end of the potential core.

Numerical calculations of the stability of axisymmetric jets described by profiles I, II and III for various values of θ will be given in the next section.

6. Numerical calculations and results for eigenvalues and eigenfunctions

Profile I: *the fully developed jet*

Batchelor & Gill (1962) demonstrated that profile I is stable to axisymmetric disturbances. Kambe (1969), Mollendorf & Gebhart (1973) and Lessen & Singh (1973) found neither neutrally stable nor amplified disturbances. The amplification factor $-\alpha_i$ is shown in figure 1 (*a*) as a function of frequency ω for several values of R. The inviscid solution is also shown. This was obtained numerically by integrating the second-order inviscid stability equation with the appropriate choice of integration contour to avoid the singularity at $U = c$. The amplification factor can be seen slowly to approach the inviscid result with increasing Reynolds number. The corresponding phase velocities are shown in figure 1 (*b*).

In order to calculate an eigenvalue using an iterative scheme it is helpful and important to find the approximate location of the eigenvalue so that the initial guesses to start the iteration allow good convergence. For any given values of the Reynolds number and frequency there will be a spectrum of eigenvalues. In stability analysis the eigenvalue whose imaginary part is algebraically the least is the most important since this is the least stable. In order to locate all the eigenvalues lying within a specified range of wavenumbers, the method used by

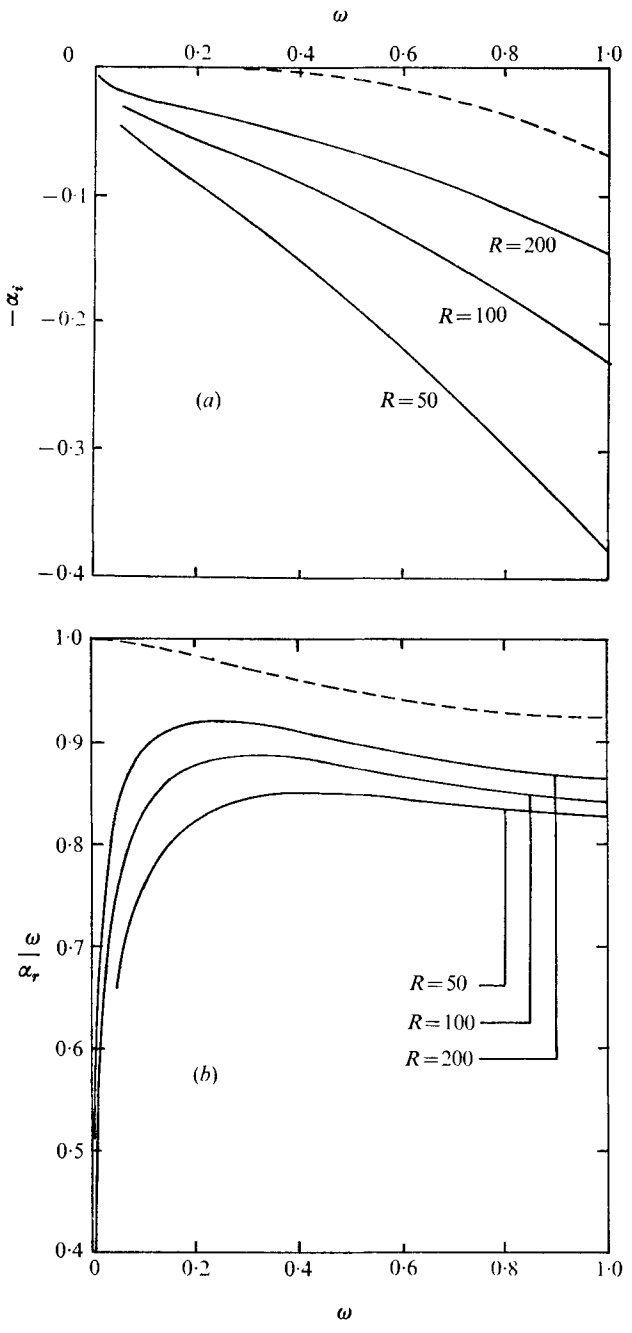

FIGURE 1. (*a*) Amplification factor and (*b*) phase velocity for mean velocity profile I; $n = 0$. – – –, inviscid calculation.

α_r	α_i
0·2322	0·0666
0·3840	0·3904
0·4842	0·8976
0·5628	1·5850

TABLE 1. Eigenvalues in the range $0 \leqslant \alpha_r \leqslant 1$, $0 \leqslant \alpha_i \leqslant 2$; $R = 80$, $\omega = 0{\cdot}2$, $n = 0$

Lessen *et al.* (1968) was adopted. By counting the number of net multiples of 2π by which the phase of Δ [equation (4.3)] changes around a closed contour in the α plane, the number of zeros within the contour may be determined. As an example the case $R = 80$, $n = 0$ and $\omega = 0{\cdot}2$ was examined. The argument of Δ altered by four net multiples of 2π around the contour $0 \leqslant \alpha_r \leqslant 1$, $0 \leqslant \alpha_i \leqslant 2$. The eigenvalues may easily be located and are given in table 1.

The eigenvalues shown in figure 1 (*a*) correspond to the least stable eigenvalues at each value of R and ω. The behaviour of the four least stable eigenvalues for $n = 0$ and $R = 80$ at low frequencies is shown in figure 2. The eigenvalues given by Mollendorf & Gebhart (1973), also shown, can be seen to refer to the first, third and fourth least stable modes. The variation of α_i with ω calculated by Lessen & Singh (1973) for two modes at $R = 75$ is also shown in figure 2. Clearly their modes II and I correspond to the third and fourth least stable modes, respectively. Thus it is clear that unless an eigenvalue search is conducted in a systematic manner, such as the method used here, important eigensolutions may be overlooked. Typical eigenfunctions for the four least stable solutions are shown in figure 3. The eigenfunctions are normalized such that $|\hat{u}| = 1$ when $r = 0$. The complexity of the eigenfunctions increases as the eigenvalue becomes more stable. The least stable eigenfunction corresponds most closely to the inviscid solution, also shown in figure 3.

The amplification factor and phase velocity as a function of ω and R for the asymmetric $n = 1$ mode are shown in figures 4(*a*) and (*b*), respectively. The phase velocity gradually approaches the inviscid solution as R increases. For the $n = 1$ mode the phase velocity increases monotonically with frequency whereas for the $n = 0$ mode (figure 1*b*) the phase velocity increased with frequency at low frequencies and decreased at high frequencies. The amplification factor does not behave in such a regular manner and an unusual phenomenon occurs. Decreasing the value of R is seen to increase the peak amplification factor as well as the amplification at low frequencies. For values of R of order less than 200 decreasing the value of R decreases the amplification factors at all frequencies. This phenomenon is not reported by Mollendorf & Gebhart (1973) but was observed by Burridge (1968) for temporal amplification, and Lessen & Singh (1973) also suggested that decreasing the Reynolds number may not provide a stabilizing influence. These calculations can be seen to lead to closed contours in the curves of constant amplification factor (figure 5).

Though the occurrence of closed contours in curves of constant amplification are not uncommon in stability analyses of flows in the presence of a boundary,

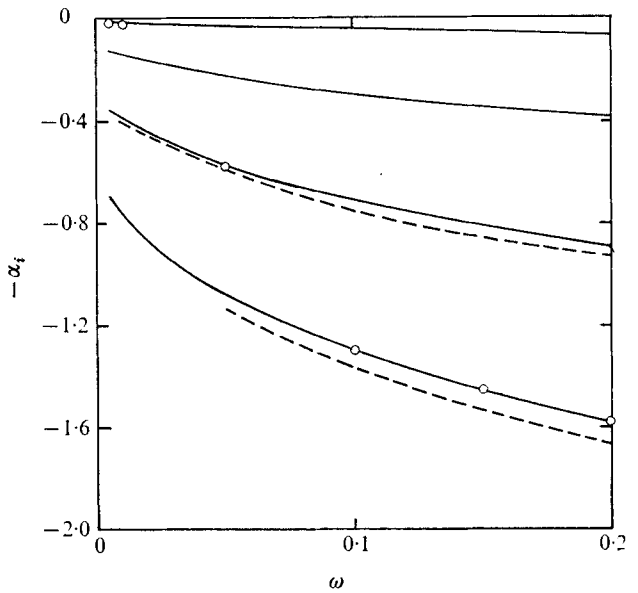

FIGURE 2. Amplification for four least stable modes for profile I; $n = 0, R = 80$. ——, present calculations; - - - -, Lessen & Singh (1973); ○, Mollendorf & Gebhart (1973).

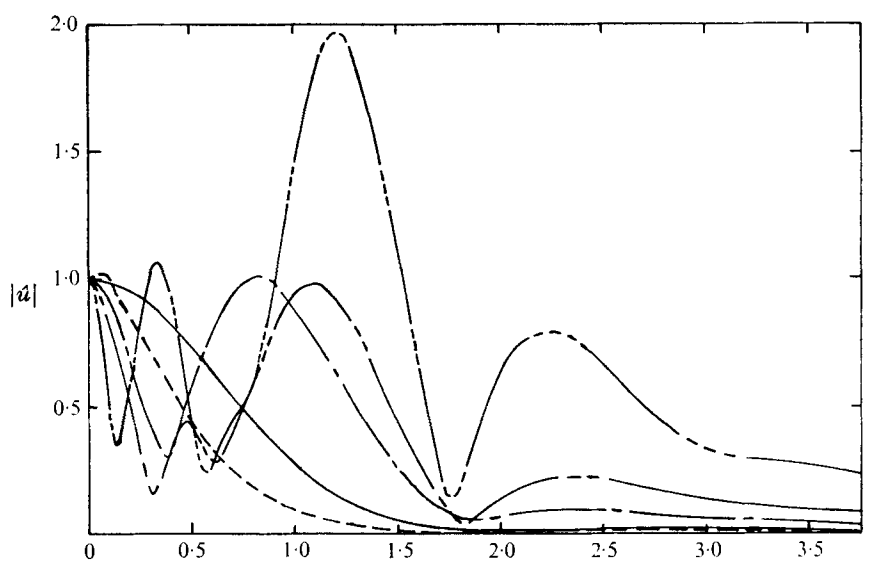

FIGURE 3. Four least stable eigenfunctions for profile I; $0 \leqslant \alpha_r \leqslant 1, R = 80, \omega = 0{\cdot}2, n = 0$. - - - - - - -, inviscid solution; ——, $\alpha = 0{\cdot}2322 + 0{\cdot}0666i$; — · —, $\alpha = 0{\cdot}3840 + 0{\cdot}3904i$; — - - —, $\alpha = 0{\cdot}4842 + 0{\cdot}8976i$; — - · - —, $\alpha = 0{\cdot}5628 + 1{\cdot}585i$.

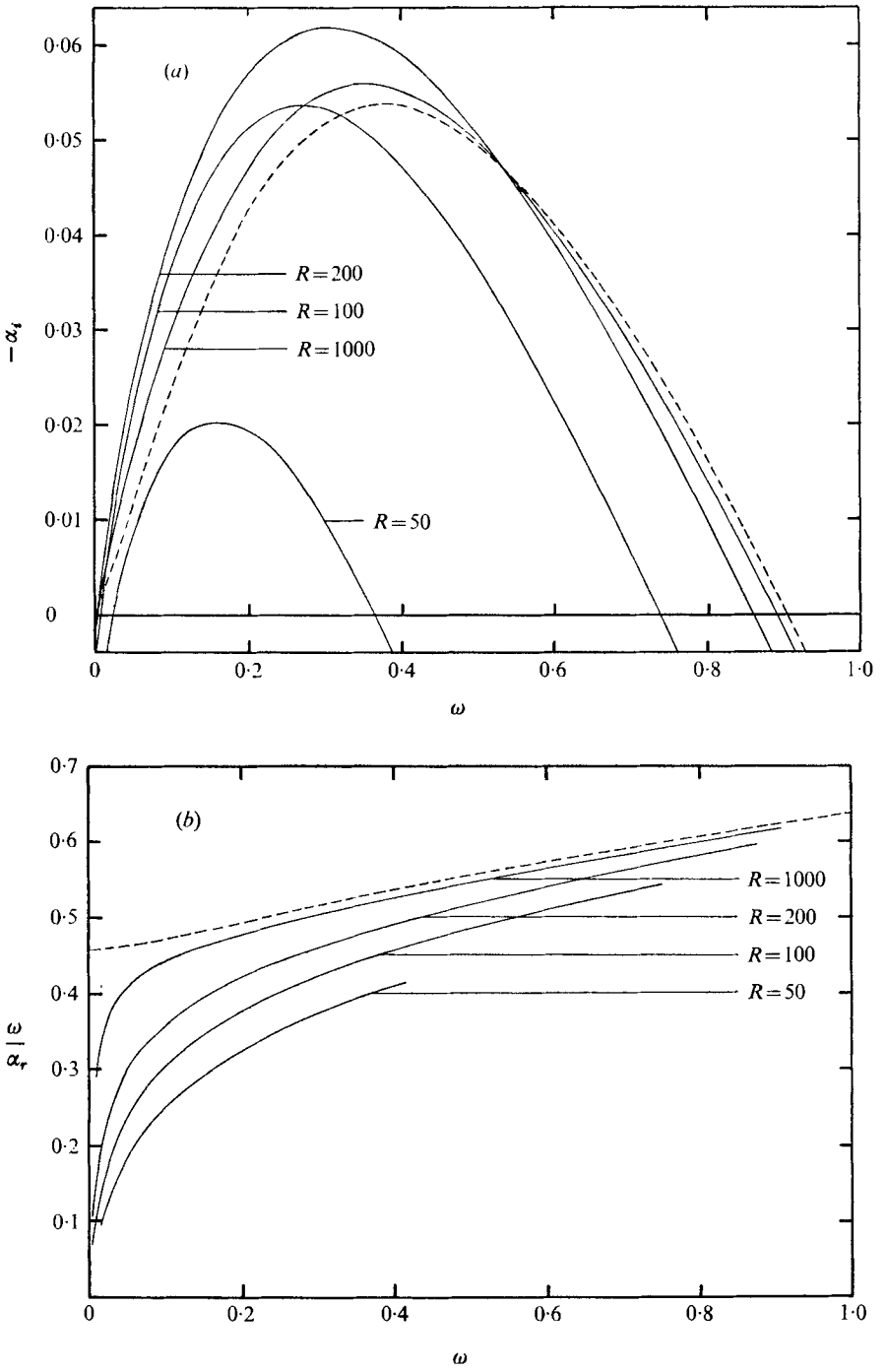

FIGURE 4. (*a*) Amplification factor and (*b*) phase velocity for mean velocity profile I; $n = 1$. - - - -, inviscid calculation.

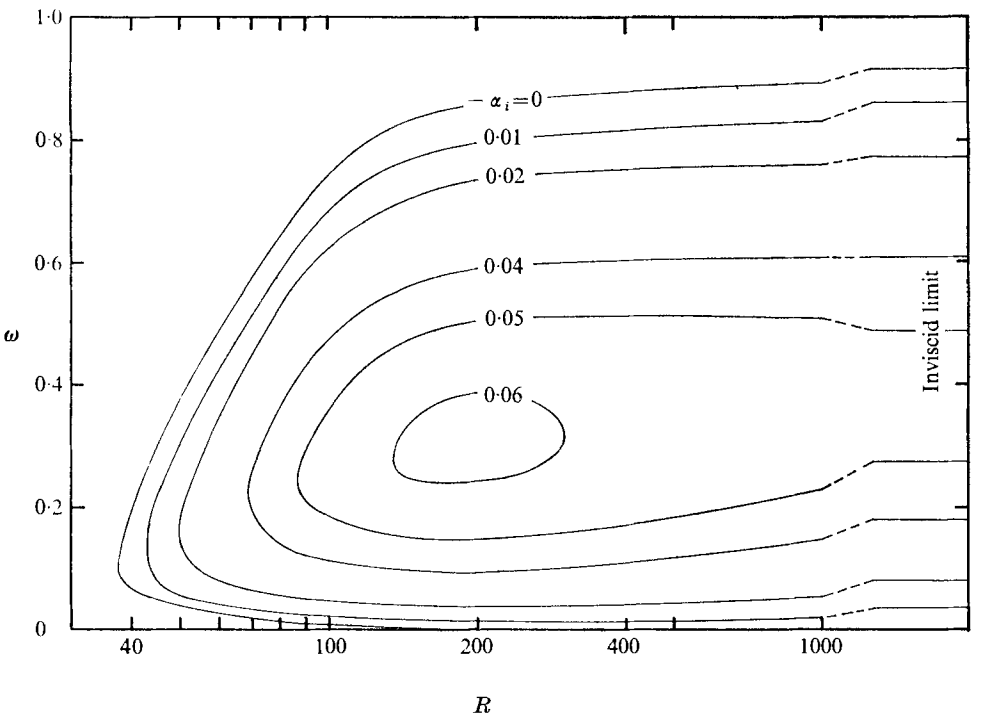

FIGURE 5. Curves of constant amplification for mean velocity profile I.

such as plane Poiseuille and Blasius flows, this occurrence is unusual in free shear flows, where a disturbance of a given wavenumber seems to have its greatest rate of growth at infinite Reynolds number (Batchelor & Gill 1962). In a very simple sense, whether a disturbance is amplified or not depends on a balance between the integrated energy production and the integrated energy dissipation. The energy production depends on the distribution of Reynolds stress and mean velocity gradient. Since the Reynolds-stress distribution is dependent on the Reynolds number, it is possible for the viscosity to affect both the viscous dissipation and the energy production. For a parallel mean flow with no axial dependence of time-averaged properties the non-dimensionalized time-averaged fluctuation energy integral equation may be written in the form

$$E^{-1}dE/dx = N - M/R, \tag{6.1}$$

where E, the integrated mechanical energy flux, is given by

$$E = \int_0^\infty \{\tfrac{1}{2}U(\overline{v^2}+\overline{w^2}+\overline{u^2})+\overline{pu}\}\,r dr, \tag{6.2}$$

N, the energy production term is given by

$$N = -\int_0^\infty \overline{uv}\frac{\partial U}{\partial r} r dr \tag{6.3}$$

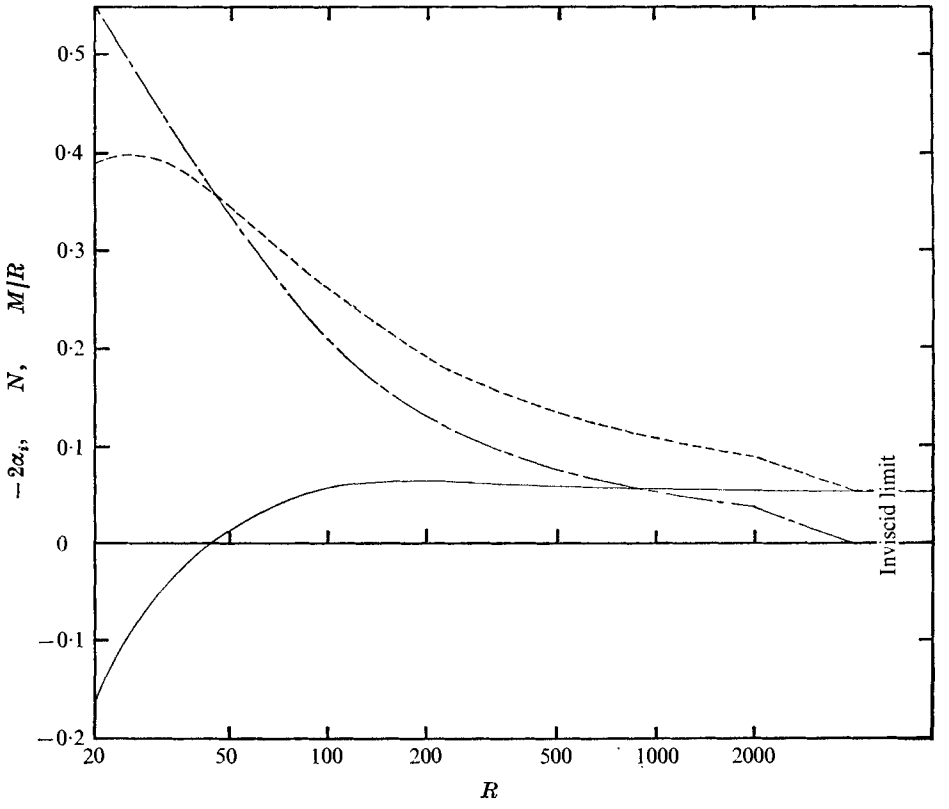

FIGURE 6. Fluctuation mechanical energy balance for profile I; $n = 1$, $\omega = 0{\cdot}3$. ——, $-2\alpha_i$; - - - - -, production, N; - — - — -, dissipation, M/R.

and M/R, the viscous dissipation, is given by

$$\frac{1}{R}\int_0^\infty \left\{ r\left[\overline{\left(\frac{\partial u}{\partial x}\right)^2} + \overline{\left(\frac{\partial u}{\partial r}\right)^2} + \overline{\left(\frac{\partial v}{\partial x}\right)^2} + \overline{\left(\frac{\partial v}{\partial r}\right)^2} + \overline{\left(\frac{\partial w}{\partial x}\right)^2} + \overline{\left(\frac{\partial w}{\partial r}\right)^2} \right] + \frac{1}{r}\left[\overline{\left(\frac{\partial u}{\partial \phi}\right)^2} + \overline{\left(\frac{\partial v}{\partial \phi}\right)^2} + \overline{\left(\frac{\partial w}{\partial \phi}\right)^2} + \overline{v^2} + \overline{w^2} + 2\overline{v\frac{\partial w}{\partial \phi}} - 2\overline{w\frac{\partial v}{\partial \phi}} \right] \right\} dr. \quad (6.4)$$

If the form of the fluctuations is assumed to be that given by (2.3) with an equivalent fluctuation amplitude $A(x)$, and the fluctuation integrals E, N, and M are normalized such that $E = |A|^2$, then (6.1) takes the form

$$-2\alpha_i = N - M/R. \quad (6.5)$$

The three terms in (6.5) are shown in figure 6 as a function of Reynolds number for $\omega = 0{\cdot}3$ and $n = 1$. Though the decrease in amplification rate from $R = 200$ to the inviscid limit is small, from $-0{\cdot}0621$ to $-0{\cdot}0518$, respectively, increasing the Reynolds number above 200 can be seen to decrease the energy production at a faster rate than the energy dissipation, giving a reduced growth or stabilizing effect.

The critical value of R was calculated to be 37·64, for $\omega = 0{\cdot}1$ and $\alpha = 0{\cdot}44$.

This agrees well with the calculations by Mollendorf & Gebhart (1973) of $R_c = 37{\cdot}6$, for $\omega = 0{\cdot}1$, by Burridge (1968) of $R_c = 37{\cdot}5$, for $\alpha = 0{\cdot}43$ and by Lessen & Singh (1973) of $R_c = 37{\cdot}9$, for $\alpha = 0{\cdot}3989$. Kambe (1969) gave a critical value of $R_c = 32{\cdot}8$ for a discontinuous parabolic mean velocity profile. Interpolation of the results of Burridge (1968) for the maximum amplification factor and use of the transformation between temporal and spatial amplification in terms of the group velocity, $(\alpha_i)_S = -(\partial\omega_r/\partial\alpha_r)\,(\omega_i)_T$ (Gaster 1962), gives a maximum value of $-\alpha_i$ of approximately 0·1 near a value of $R = 200$. This value is somewhat higher than that given by the direct spatial stability calculation. However the transformation is only valid for small rates of amplification. The corresponding eigenfunctions are also found to agree closely with those of Mollendorf & Gebhart (1973) and Lessen & Singh (1973).

Profile II: *the initial mixing region*

The inviscid stability equation for this mean velocity profile has been solved by Michalke (1971) for amplifying disturbances only. The amplification factors and phase velocities for the axisymmetric ($n = 0$) mode are shown in figures 7 (*a*) and (*b*), respectively. The wavenumber, frequency and Reynolds number are each expressed as a local quantity by multiplying each by the local non-dimensional thickness θ. As a check on the numerical series expansions for profiles II and III, the initial values in the numerical integration were obtained separately using both the series expansions for constant mean velocity and the analytic form of the solutions (3.5). Both methods gave the same answer to within four significant figures. The maximum amplification in the inviscid solution, for small values of θ, approaches the result for the two-dimensional shear layer, given by Michalke (1965), of $\omega = 0{\cdot}1034$, $\alpha_r = 0{\cdot}2015$ and $\alpha_i = -0{\cdot}1142$. In these calculations for the axisymmetric mixing region and $\theta = 0{\cdot}02$, it is found that for maximum amplification $\omega\theta = 0{\cdot}108$, $\alpha_r\theta = 0{\cdot}199$ and $\alpha_i\theta = -0{\cdot}114$. At low frequencies the phase velocity exceeds the jet centre-line velocity by as much as 30 %. This is observed for both the inviscid and the viscous solutions. The value of this peak increases with increasing Reynolds number up to a value of $R\theta$ of the order of 10 before approaching the inviscid limit with a further increase in $R\theta$.

The $n = 1$ mode is found to exhibit very similar amplification rates to the $n = 0$ mode except at low frequencies, where it is marginally less stable. The phase velocities for the $n = 1$ mode are found to be always less than the jet velocity.

The critical Reynolds numbers for the first two modes for $\theta = 0{\cdot}02$ are

$$R_c\theta = 0{\cdot}683, \quad \omega\theta = 0{\cdot}0233, \quad \alpha\theta = 0{\cdot}0313 \quad \text{for} \quad n = 0,$$
$$R_c\theta = 0{\cdot}444, \quad \omega\theta = 0{\cdot}0070, \quad \alpha\theta = 0{\cdot}0149 \quad \text{for} \quad n = \theta.$$

Thus, close to the jet exit, though the maximum inviscid amplification rates are similar the critical Reynolds number for the $n = 1$ mode is marginally less than that for the $n = 0$ mode.

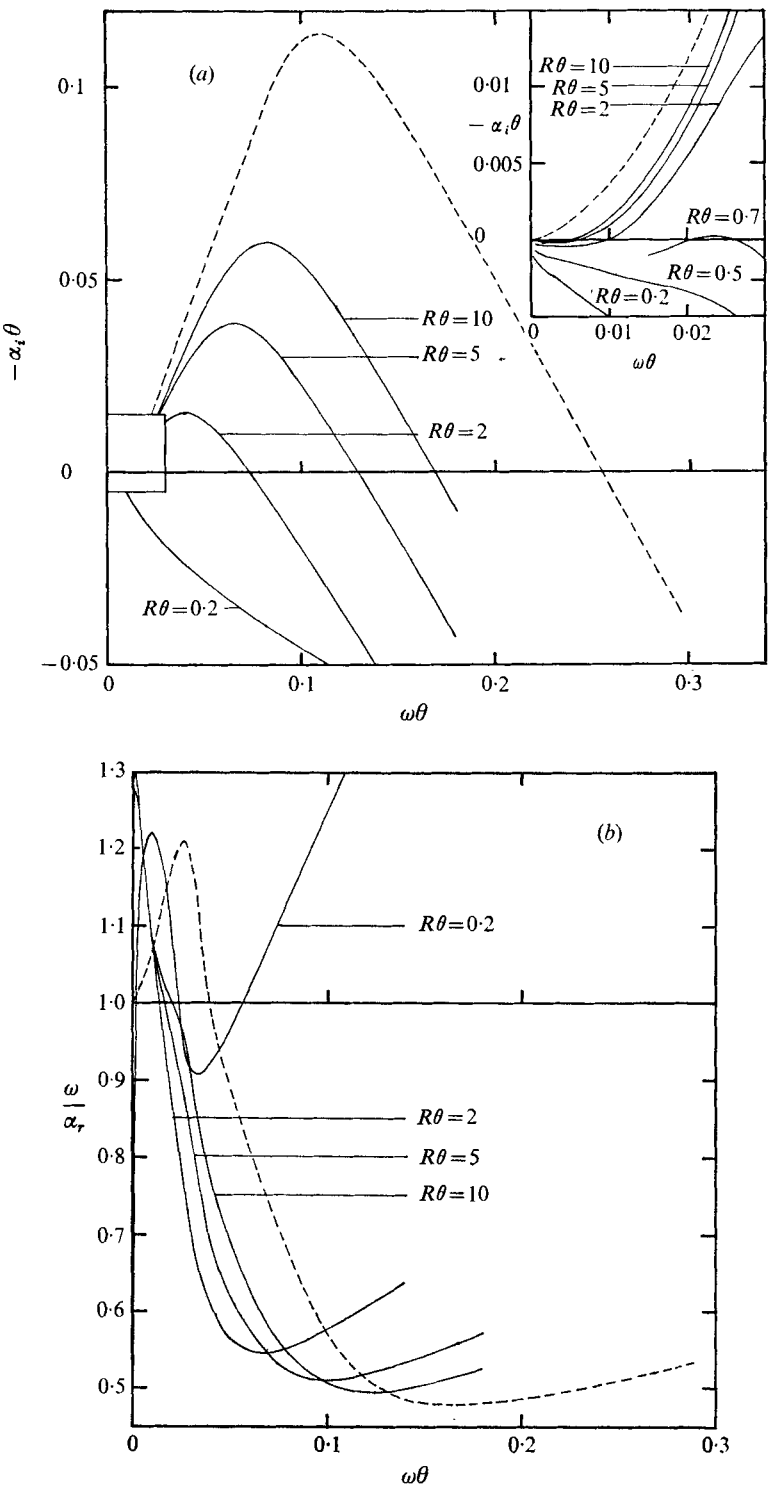

FIGURE 7. (*a*) Amplification factor and (*b*) phase velocity for mean velocity profile II; $\theta = 0{\cdot}02$, $n = 0$. ----, inviscid calculation.

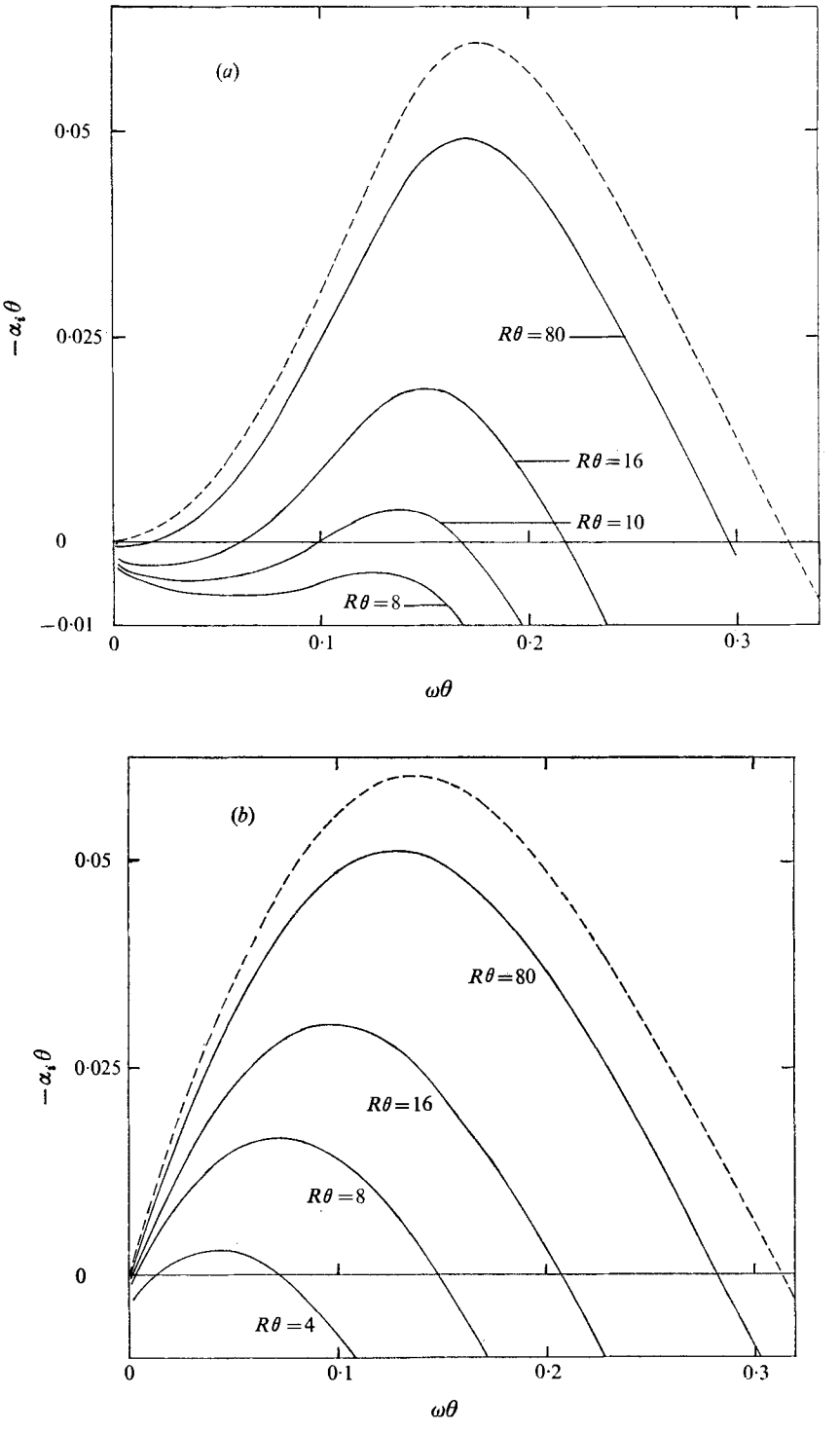

FIGURE 8. Amplification factor for mean velocity profile III; $\theta = 0{\cdot}16$. (*a*) $n = 0$. (*b*) $n = 1$. – – –, inviscid calculation.

Profile III: *the developed annular mixing region*

The amplification factors for the axisymmetric ($n = 0$) mode are shown in figure 8(a). For finite Reynolds number these do not exceed the inviscid limiting values and behave in a similar manner to those for profile II or the two-dimensional shear layer. The corresponding phase velocity is found to tend to the inviscid limit from above at high frequencies. At low frequencies, however, increasing the Reynolds number leads to an increase in the peak phase velocity, which is in excess of the jet velocity, at a decreasing value of the frequency.

The amplification rates for the $n = 1$ mode are shown in figure 8(b). The maximum amplification for the $n = 1$ mode occurs at a lower frequency than that for the $n = 0$ mode. At low frequencies the $n = 1$ mode is more unstable than the $n = 0$ mode. For $R\theta > 10$ and $\omega\theta > 0{\cdot}2$, the axisymmetric mode is slightly less stable. The phase velocity for the inviscid $n = 1$ mode varies only slightly with frequency and lies between 0·6 and 0·7 of the jet exit velocity. Decreasing the Reynolds number leads to a reduction in phase velocity at low frequencies and an increase in phase velocity at high frequencies.

The critical Reynolds numbers for the first two modes for $\theta = 0{\cdot}16$ are

$$R_c\theta = 8{\cdot}85, \quad \omega\theta = 0{\cdot}1324, \quad \alpha\theta = 0{\cdot}1645 \quad \text{for} \quad n = 0,$$

$$R_c\theta = 3{\cdot}48, \quad \omega\theta = 0{\cdot}0349, \quad \alpha\theta = 0{\cdot}0914 \quad \text{for} \quad n = 1.$$

7. Discussion

From the preceding calculations it is possible to show how a disturbance of constant physical frequency develops as it propagates downstream. For a flow where the mean velocity is a function of both radial and axial distance an equation of the form (6.1) may be developed which includes the axial dependencies. If the fluctuations in the analogous equation are approximated by local eigensolutions obtained assuming infinite parallel flow with the local mean velocity profile, an assumption which becomes more accurate as the Reynolds number increases, then the disturbance mean-square amplitude at any axial position may be related to its initial value by the expression

$$|A|^2/|A|_0^2 = \exp\left\{-2\int_0^z \alpha_i dz\right\}. \tag{8.1}$$

Clearly the local amplitude depends on both the initial amplitude and the variation of growth rate with axial distance. Examination of the amplification rates in the annular mixing region shows that for a fixed frequency ω increasing the thickness θ leads first to increasing and then to decreasing amplification and finally to damping. Thus at each axial position the frequency of the disturbance that is most amplified will differ and will decrease with increasing axial distance. Correspondingly, the axial location of maximum amplitude for a disturbance of given constant physical frequency, given by the location at which $\alpha_i = 0$, will also move downstream with decreasing frequency. It can also be seen from the present

calculations that only the $n = 1$ mode can grow in the developed jet flow. Thus the location of peak amplitude of any axisymmetric disturbance will occur before this profile is encountered. The helical mode ($n = 1$) for low frequencies will continue to amplify in the developed jet flow. However it should be noted that in this region the disturbances are non-dimensionalized with respect to the jet centre-line velocity, so that a helical disturbance may decrease in absolute amplitude even though the local eigenvalue suggests amplification.

The present calculations also indicate why there exist discrepancies between the experimentally observed modes of instability: some are axisymmetric, some helical. For a mean velocity profile given by a one-sided Gaussian distribution the inviscid analysis of Mattingly & Chang (1974) showed that the axisymmetric mode was the most unstable close to the jet exit. For the hyperbolic-tangent profile used in the present calculations to represent the mean flow profile close to the jet exit the inviscid calculations show nearly identical maximum growth rates for the $n = 0$ and $n = 1$ modes. Thus the smallest change in initial mean velocity profile can be expected to lead to different observations. The observed mode of instability will also depend on the initial perturbation, whether this is naturally occurring or excited. If the axisymmetric mode has the greatest initial amplitude at the jet exit, perhaps caused by a small fluctuation in the jet velocity, it will dominate in the first few diameters downstream. However if both axisymmetric and helical modes have nearly equal amplitudes then the helical mode will tend to dominate downstream of the end of the potential core.

The Reynolds number referred to in this paper for profile I is based on the momentum flux of the jet and so the relationship between this Reynolds number and that based on jet exit conditions depends on the velocity profile at the jet exit. In Reynolds' (1962) experiments $Re_D = Qd/A\nu$, where Q is the volume flow through the nozzle and A is the nozzle area. Thus, for a parabolic profile at the jet exit $Re_D = R$ and for a top-hat profile $Re_D = (2/3\frac{1}{2})R$. Thus the critical Reynolds numbers determined for the $n = 1$ mode in these calculations, given in terms of Reynolds' (1962) experimental Reynolds numbers, are $Re_D = 43{\cdot}6$ and $Re_D = 37{\cdot}64$ for uniform and parabolic jet exit flows respectively. These values are lower than the observed first occurrences of the sinuous mode of instability by Reynolds (1962) at an Re_D of about 100. However, as suggested by Lessen & Singh (1973), no correction has been made for flow divergence, which may or may not be stabilizing.

This work was sponsored by Air Force Contract F33615-73-C-2032, which is jointly funded by the Air Force Aero Propulsion Laboratory and the U.S. Department of Transportation.

REFERENCES

ANDRADE, E. N. D. & TSIEN, L. C. 1937 The velocity distribution in a liquid-into-liquid jet. *Proc. Phys. Soc. Lond.* **49**, 381.

BATCHELOR, G. K. & GILL, A. E. 1962 Analysis of the stability of axisymmetric jets. *J. Fluid Mech.* **14**, 529.

BELLMAN, R. E. & KALABA, R. E. 1965 *Quasi-linearization and Non-linear Boundary-value Problems*. Elsevier.

BURRIDGE, D. M. 1968 The stability of round jets. Ph.D. thesis, Bristol University.

CONTE, S. D. 1966 The numerical solution of linear boundary-value problems. *SIAM Rev.* **8**, 309.

CRIGHTON, D. G. 1973 Instability of an elliptic jet. *J. Fluid Mech.* **59**, 665.

CROW, S. C. & CHAMPAGNE, F. M. 1971 Orderly structure in jet turbulence. *J. Fluid Mech.* **48**, 547.

DAVEY, A. 1973 A simple numerical method for solving Orr–Sommerfeld problems. *Quart. J. Mech. Appl. Math.* **26**, 401.

DAVEY, A. & NGUYEN, H. P. F. 1971 Finite-amplitude stability of pipe flow. *J. Fluid Mech.* **45**, 701.

FREYMUTH, P. 1966 On transition in a separated laminar boundary layer. *J. Fluid Mech.* **25**, 683.

FYFE, D. J. 1966 Economical evaluation of Runge–Kutta formulae. *Math. Comp.* **20**, 392.

GARG, V. K. 1971 Stability of pipe Poiseuille flow to infinitesimal disturbances. Ph.D. thesis, Carnegie-Mellon University Pittsburgh.

GARG, V. K. & ROULEAU, W. T. 1972 Linear spatial stability of pipe Poiseuille flow. *J. Fluid Mech.* **54**, 113.

GASTER, M. 1962 A note on the relation between temporally-increasing and spatially-increasing disturbances in hydrodynamic stability. *J. Fluid Mech.* **14**, 222.

GILL, A. E. 1962 On the occurrence of condensations in steady axisymmetric jets. *J. Fluid Mech.* **14**, 557.

GILL, A. E. 1965 On the behaviour of small disturbances to Poiseuille flow in a circular pipe. *J. Fluid Mech.* **21**, 145.

KAMBE, T. 1969 The stability of an axisymmetric jet with a parabolic profile. *J. Phys. Soc. Japan*, **26**, 566.

LANDAU, L. D. & LIFSHITZ, E. M. 1959 *Fluid Mechanics*. Pergamon.

LESSEN, M., SADLER, S. G. & LIU, T.-Y. 1968 Stability of pipe Poiseuille flow, *Phys. Fluids*, **11**, 1404.

LESSEN, M. & SINGH, P. J. 1973 The stability of axisymmetric free shear layers. *J. Fluid Mech.* **60**, 443.

MATTINGLY, G. E. & CHANG, C. C. 1974 Unstable waves on an axisymmetric jet column. *J. Fluid Mech.* **65**, 541.

MICHALKE, A. 1965 On spatially growing disturbances in an inviscid shear layer. *J. Fluid Mech.* **23**, 521.

MICHALKE, A. 1971 Instabilität eines kompressiblen runden Freistrahls unter Berücksichtigung des Einflusses der Strahlgrenzschichtdicke. *Z. Flugwiss.* **19**, 319.

MOLLENDORF, J. C. & GEBHART, B. 1973 An experimental and numerical study of the viscous stability of a round laminar vertical jet with and without thermal buoyancy for symmetric and asymmetric disturbances. *J. Fluid Mech.* **61**, 367.

MORRIS, P. J. 1971 The structure of turbulent shear flow. Ph.D. thesis, Southampton University.

ORSZAG, S. A. & CROW, S. C. 1970 Instability of a vortex sheet leaving a semi-infinite plate. *Stud. Appl. Math.* **49**. 167.

PAI, S. I. & HSIEH, T. 1972 Numerical solution of laminar jet mixing with and without free stream. *Appl. Sci. Res.* **27**, 39.

REYNOLDS, A. J. 1962 Observations of a liquid-into-liquid jet. *J. Fluid Mech.* **14**, 552.

SHARMA, R. 1968 The structure of turbulent shear flow. Ph.D. thesis, Southampton University.

VIILU, A. 1962 An experimental determination of the minimum Reynolds number for instability in a free jet. *J. Appl. Mech.* **29**, 506.